applied sciences

MDPI

Article

Experimental Study on the Bearing Capacity of Gas Oil-Contaminated Coastal Sand

Ali Khezri [1], Mohamadali Moradi [2], Hongbae Park [3] and Daeyong Lee [3,*]

[1] Energy Innovation Research Center for Wind Turbine Support Structures, Kunsan National University, 558 Daehak-ro, Gunsan-si 54150, Jeollabuk-do, Republic of Korea; ali94kzr@kunsan.ac.kr
[2] Department of Civil and Environmental Engineering, Amirkabir University of Technology, Tehran 15875-4413, Iran; ma.moradi@aut.ac.ir
[3] Department of Wind Energy, The Graduate School of Kunsan National University, 558 Daehak-ro, Gunsan-si 54150, Jeollabuk-do, Republic of Korea; dcv003@naver.com
* Correspondence: daeyong.lee@kunsan.ac.kr

Abstract: Ground hydrocarbon contamination is a grave consequence of fossil fuel consumption, making it increasingly unsustainable. Consequently, researchers worldwide have been compelled to conduct a large number of studies on the geotechnical aspects of hydrocarbon-contaminated soils. Still, the complications arising from the integration of geotechnical complexities with diverse hydrocarbon properties present a substantial research need. The assessment of the foundation bearing capacity in hydrocarbon-contaminated soils is of paramount importance, especially given that numerous contaminated sites either house significant industrial facilities or are earmarked for critical infrastructure projects. This study investigates the shear strength and bearing capacity of gas oil-contaminated coastal sands using laboratory testing and physical modeling, with a special focus on the combined influence of the degree of saturation and relative density. Footing's shear failure mechanisms were analyzed based on predicted and measured bearing capacity values. Findings show a decrease in the friction angle with a contamination increase, while the apparent cohesion initially rises before declining. Furthermore, the study revealed that the foundation's bearing capacity exhibited an increase up to a specific contamination level, followed by a subsequent decrease. This increase is circa 90 and 100 percent at a 5 percent contamination content for loose and dense sand, respectively. Comparing the predicted and measured bearing capacity results shows that the general shear failure mechanism has occurred in the dense subgrade, while the loose subgrade's failure mechanism is more inclined towards local shear failure.

Keywords: contaminated soils; sand; sustainability; environmental geotechnics; bearing capacity

check for updates

Citation: Khezri, A.; Moradi, M.; Park, H.; Lee, D. Experimental Study on the Bearing Capacity of Gas Oil-Contaminated Coastal Sand. *Appl. Sci.* **2023**, *13*, 12450. https://doi.org/10.3390/app132212450

Academic Editor: Dongmei Zhou

Received: 12 October 2023
Revised: 9 November 2023
Accepted: 15 November 2023
Published: 17 November 2023

Copyright: © 2023 by the authors. Licensee MDPI, Basel, Switzerland. This article is an open access article distributed under the terms and conditions of the Creative Commons Attribution (CC BY) license (https://creativecommons.org/licenses/by/4.0/).

1. Introduction

In the last century, onshore and offshore oil spills and continuous oil leakage to the ground have become challenging issues worldwide. From about two million tons of oil produced daily, 10% enter the environment due to the breakdown of petroleum production facilities, transportation accidents, and reservoir leakage, to name a few [1]. The destruction of Kuwait's oil production facilities at the end of the Gulf War [2] and the 2007 Korean oil spill are examples of onshore and coastal oil pollution of vast proportions. Besides the environmental hazards and ecological damage, oil contamination can change the mechanical properties of the soil and, consequently, alter the bearing capacity of the foundations. Onshore/offshore oil spills and reservoir leakages often occur in sites with industrial significance, such as coastal areas housing diverse industries, including wind farms, petrochemical industries, and ports [3]—see Figure 1. Such infrastructure often involves heavy, high-rise structures relying on foundations sensitive to bearing capacity alteration.



(**a**) (**b**)

Figure 1. (**a**) Yeonggwang wind power farm; (**b**) HD Hyundai Oilbank's Daesan plant.

In the Republic of Korea, for instance, several oil spill incidents—including the Hebei Spirit crude oil spill in 2007 and the Sea Prince accident in 1955, which contaminated over 200 and 73 km of coastline, respectively—have induced major oil contamination in sites of high industrial prominence [4,5]. These incidents are on top of the numerous oil leakages occurring in terrestrial environments due to industrial and petrochemical activities [6].

In the last decades, a number of reduced-scale physical modeling [7–11], laboratory element testing [1,2,12–21], and field testing [22] studies have been conducted to study the variations in the mechanical properties of soils contaminated with different types of contaminants. Al-Sanad et al. [2] conducted one of the first comprehensive laboratory studies on oil-contaminated soils using Kuwaiti Jahara sand samples. They found a slight reduction in the friction angle compared to clean sand. CBR test results showed a 25% increase with 4% oil content, which then dropped at 6% oil content. In a study by Shin and Das [7] on contaminated Jumoonjun sand (east coast of the Republic of Korea), they observed a decrease in the bearing capacity as the contamination levels increased. In their 2007 study, Khamehchiyan et al. [20] examined the impact of crude oil contamination on coastal soil samples from Bushehr, Iran (SM, SP, and CL types). Their results showed that, as the oil content increased, the friction angle and cohesion of the SP and SM samples decreased and increased, respectively.

Abtahi and Boushehrian [10] examined the impact of the contamination type and depth on the bearing capacity of a circular footing. Their findings revealed a reduction in bearing capacity due to oil contamination. Furthermore, Nasehi et al. [13] investigated the impact of gas oil contamination on SP, ML, and CL soil samples using basic laboratory tests, including unconfined compression strength (UCS) and direct shear tests. Their findings indicated that the friction angle decreased and the cohesion increased with the contamination level. Additionally, the UCS results revealed that the strength of CL samples increased with 3% contamination. Alhassan and Fagge [19] assessed the strength properties of hydrocarbon-contaminated soil samples. They conducted tests on three soil samples, each contaminated with a different type of hydrocarbon (see Table 1). Their findings revealed that the CBR value and shear strength of both sand and laterite samples initially increased with the contamination content up to a certain point, after which they started to decrease. Rajabi and Sharifipour [23] studied the short- and long-term effects of light crude oil contamination on the maximum shear modulus of Firoozkoh and Ottawa sand using bender element testing. Their findings revealed that the introduction of 4% crude oil into both soil types significantly increased the small-strain shear modulus. However, further contamination led to a notable decrease in the maximum shear modulus (G_{Max}).

In light of the literature, it can be noticed that changes in soil strength due to hydrocarbon contamination depend significantly on the specific properties of both hydrocarbons and the soil. In the majority of the cited studies, very limited focus has been allocated to the unsaturated behavior of hydrocarbon-contaminated soils, which can be greatly influential on the strength properties and bearing capacity of soils. This approach is also commonly adopted in the estimation of the bearing capacity and settlement of shallow foundations rested atop unsaturated soils [24,25]. Such approaches, which are based on a worst-case scenario, may not represent the realistic condition for many shallow foundations and consequently can lead to an uneconomical foundation design [26–29].

Table 1. A summary of studies on geotechnical properties of hydrocarbon-contaminated soils.

Research	Average Particle Size, *D*50 mm	Contamination Type	Classification (Unified)	Bearing Capacity	CBR	Friction Angle	Cohesion
AI-Sanad et al. (1995) [2]	0.43	Heavy and Light Crude Oil, Benzene, Gas Oil	SP	-	Increase *	Decrease	-
Srivastava and Pandy (1998) [16]	0.04	Crude Oil	Sand	-	-	Decrease	Increase *
Shin and Das (2001) [7]	0.6	Oman Crude Oil	SP	Decrease	-	Decrease	-
Khamehchiyan et al. (2007) [20]	0.28	Crude Oil	SP	-	-	Decrease	Increase *
	0.14		SM	-	-	Decrease	Increase
	0.01		CL	-	-	Increase	Decrease
Nasr (2009) [8]	0.52	Heavy Motor Oil and Light Gas oil	SP	Decrease	-	-	-
Puri (2000) [12]	Not Reported (D10 = 0.15)	Crude Oil	SP	-	-	Decrease	-
Kermani and Ebadi (2012) [1]	0.018	Crude Oil	CL	-	-	Increase	Decrease
Khosravi et al. (2013) [15]	<0.01	Gas oil	CL	-	-	Decrease	Increase
Alhassan and Fagge (2013) [19]	99% < 0.315 mm	Crude Oil	SP		Increase *	Shear Strength: Increase *	
	100% < 0.315 mm	LPFO	SC	-	Decrease	Shear Strength: Constant	
	82% < 0.315 mm	Vacuum Gas Oil	Laterite		Increase *	Shear Strength: Increase *	
Akinwumi (2014a) [17]	0.05	Nigerian Crude Oil	Sandy Lean	-	Increase *	-	-
Akinwumi (2014b) [18]	0.05		Clay	-	Increase *	-	-
Nasehi et al. (2015) [13]	0.6	Gas oil	SP	-	-	Decrease	Increase *
	0.035		ML	-	-	Decrease	Increase
	0.026		CL	-	-	Decrease	Increase
Abtahi and Boushehrian (2020) [10]	1.2	Gas oil Kerosene	SP	Decrease	-	Decrease	Increase Increase
Kererat (2019) [22]	0.36	Gasoline	SM	Decrease	-	Decrease	Increase *
Joukar and Boushehrian (2020) [9]	1.2	Gas oil Kerosene	SP	Decrease	-	Decrease	Increase Increase
Ahmadi and Ebadi (2021) [14]	≈0.2	Crude Oil	SP-SC	-	-	Decrease	Increase
	<0.2		SC-SM	-	-	Decrease	Increase
	<<0.2		CL-ML	-	-	Increase	Increase *

* Increase to a specific saturation level, and then a decrease.

Considering the literature outlined in Table 1, it becomes evident that only a limited number of studies have addressed the bearing capacity of hydrocarbon-contaminated soils. These studies often concentrated on coarse-grained sand with a single relative density and a limited range of degree of saturation. In contrast, our present study seeks to investigate the bearing capacity and strength characteristics of fine-grained coastal sand contaminated with hydrocarbons under different relative densities and contamination levels. Fine-grained natural sand not only mirrors the type of sand commonly found in coastal areas where major industries are located but also facilitates the exploration of prominent unsaturated behaviors, such as soil suction.

The combined influence of the degree of saturation and relative density is known to greatly affect the failure mode of the foundation's subgrade [26]. Therefore, our research aims to provide insight into the transition in the failure modes influenced by unsaturated conditions and the relative density. Our approach utilizes a physical model to determine the foundation bearing capacity across different subgrade conditions and corroborates these results with direct shear tests. The study ultimately compares the predicted bearing capacity with the measured values based on these experiments.

2. Laboratory Investigation

2.1. Materials

A typical fine-grained, gap-graded coastal sand was selected to be used in this study. The physical properties of the sand and its grain size distribution are presented in

Table 2 and Figure 2, respectively. The Chamkhale sand (from the coastline of the Caspian Sea) is classified as poorly graded (SP) according to the Unified Soil Classification System. The median particle size of the sand (i.e., D50) is 0.175 mm; therefore, no particle size effect on the results of the physical modeling is expected, as it provides a footing width (B) to median particle size (B/D50) of greater than 850, which is well above the minimum ratio recommended for avoiding possible particle size effects [30]. Drawing from records of hydrocarbon contaminations that occurred on the west coast of the United States between 2002 and 2015, Rajabi and Sharifipour [31] identified gas oil as one of the most prevalent ground pollutants. Consequently, in our current study, we have selected gas oil as the focus of our soil contamination investigation. The key properties of gas oil are outlined in Table 3 for reference.

Table 2. Properties of the sand used in the model tests.

Property	Standard	Value
Specific gravity, *Gs*	ASTM D-854 [32]	2.7
Unified Soil Classification	ASTM D-2488 [33]	SP
*D*10 mm		0.115
*D*30 mm		0.165
*D*50 mm		0.17
*D*60 mm		0.18
Uniformity coefficient, *Cu*	ASTM D-2488 [33]	1.57
Coefficient of curvature, *Cc*	ASTM D-2488 [33]	1.31
Maximum dry unit weight, $(\gamma_d)_{max}$ kN/m^3	ASTM D-4253 [34]	13.55
Maximum void ratio, e_{max}		0.95
Minimum dry unit weight, $(\gamma_d)_{min}$ kN/m^3	ASTM D-4254 [35]	15.95
Minimum void ratio, e_{min}		0.66

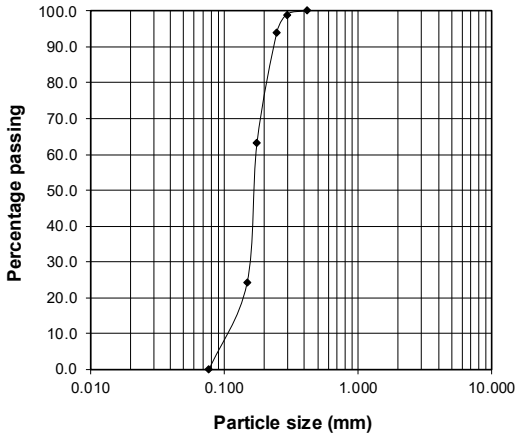

Figure 2. Particle size distribution of the sand.

Table 3. Gas oil properties.

Property	Standard	Value
Density in 15 °C (kN/m^3)	ASTM D1298 [36]	8.2–8.6
Kinematics viscosity $10^{-6} \times$ m^2/s (c.St)	ASTM D445 [37]	2.0–5.5 (max)
Fuel boiling point, F.B.P. (°C)	ASTM D86 [38]	385 (max)
Fuel flash point, F.F.P. (°C)	ASTM D93 [39]	54 (min)

2.2. Direct Shear Tests

A direct shear test apparatus was employed to determine the shear strength of the soil samples. Samples were prepared in a 10 × 10 × 3 cm shear box with four distinct initial gas oil contents: 0%, 5%, 10%, and 15%. The samples were sheared at a constant rate of 1 mm/min under vertical stresses of 50 kPa, 100 kPa, and 200 kPa, in accordance with ASTM D3080

guidelines. Before placing the soil into the box, the sand was mixed with a specific gravimetric gas oil content to achieve the desired level. To account for evaporation and gas oil loss during preparation, a slightly greater amount of gas oil was added to the mixture.

After transferring the soil samples into the shear box, we employed the wet-tamping method to achieve specific relative densities of 30% and 70% at varying initial degrees of saturation. The control of the relative densities was accomplished through precise measurements of the specimen height in the direct shear box for a given specimen weight.

For sandy soil, previous studies, including those by Verdugo and Ishihara [40] and Wood et al. [41], have indicated that sample preparation effects, such as alterations in the soil mass structure, predominantly arise from the preparation methods employed, such as wet tamping, water sedimentation, and air pluviation. It is worth noting that minimal structural changes are expected when a single preparation method is utilized. Additionally, Verdugo and Ishihara [40] have pointed out that structural differences primarily impact the small-strain behavior of sandy soil, with large-strain behavior being less influenced due to the elimination of the soil structure at large strains. Consequently, similar strength properties are anticipated at large strains. Furthermore, Wood et al. [41] have concluded that the behavior of dense silty sand remains largely unaffected by the sample preparation method, though some effects may be observed when there is an increase in the silt content within the sand mass. The sand used in the present study lacks fine-grain silt; the results are obtained in large strains, and we exclusively employed the wet-tamping method for sample preparation. Therefore, it is reasonable to assume that no significant sample preparation effects are expected in these tests.

2.3. Physical Modeling Tests

Reduced-scale tests offer precise control for studying foundation behavior but require careful interpretation due to "scale effects" arising from (I) foundation stress on the subgrade, (II) the footing size relative to the soil grains, (III) soil anisotropy affecting the failure plane orientation, and (IV) progressive failure and nonuniform soil strains.

Among the mentioned effects, the difference in the stress level between reduced- and full-scale footings, as highlighted by Lau and Bolton [30], is of paramount significance. Larger footings generate greater stress within their influence zone. Due to the nonlinearity of the Mohr–Coulomb (MC) failure envelope—resulting in higher φ values at lower stress levels—the friction angle at failure is greater in reduced-scale footings compared to full-scale footings [42]. Several strategies have been proposed in prior studies to account for these scale effects. Lau and Bolton [30] suggested determining the N_γ factor based on friction angles as a function of the applied pressure. Additionally, Zhu et al. [43], Shiraishi [44], and Cerato and Lutenegger [45] advocated adopting N_γ values based on the footing size. Another influential factor affecting the bearing capacity is the ratio of the footing width (B) to the median grain size of the soil particles (B/D50). To mitigate particle size effects, Kusakabe [46] recommends maintaining a minimum B/D50 ratio of 50–100.

Furthermore, in the case of unsaturated subgrades, the distribution of suction (or the saturation level) should be considered when interpreting the results of the physical modeling of shallow footings. In such subgrades, the average matric suction should be considered in the determination of the bearing capacity, which may be a function of the footing dimension, as larger foundations influence the underneath soil to greater depth and may have a different average matric suction compared to smaller foundations. Nonetheless, in case the profile of the matric suction distribution is uniform in depth, the average matric suction will be constant for different foundation sizes [47,48].

The above-mentioned scaling effects were taken into account in the physical model experiments in the present research. As previously mentioned in Section 2.1, grain size effects are not an issue in this study, as the ratio is well above the recommended value. Moreover, subgrade layers were prepared with a uniform profile of degree of saturation in depth in order to achieve a constant average degree of saturation in all layers. The

foundation width effect is also considered in the determination of the N_γ values and interpretation of the predicted bearing capacity results in Section 4.

The physical modeling tests were conducted in the soil dynamics laboratory at the Amirkabir University of Technology. These experiments utilized a rectangular tank as the foundation subgrade container, with specific dimensions of 100 × 80 × 65 cm (length × width × height), as illustrated in Figure 3. The tank's interior featured a smooth, impermeable membrane to prevent gas oil leakage and minimize friction between the tank wall and sand grains. The foundation model consisted of a 2 cm thick, 15 cm wide square steel plate. Given the stress levels in the bearing capacity tests, the foundation exhibited a rigid response. An abrasive sheet was affixed to the foundation's bottom to replicate the friction between an actual concrete foundation and its subgrade. All tests were conducted with the foundation placed on the subgrade surface without any embedment considered.

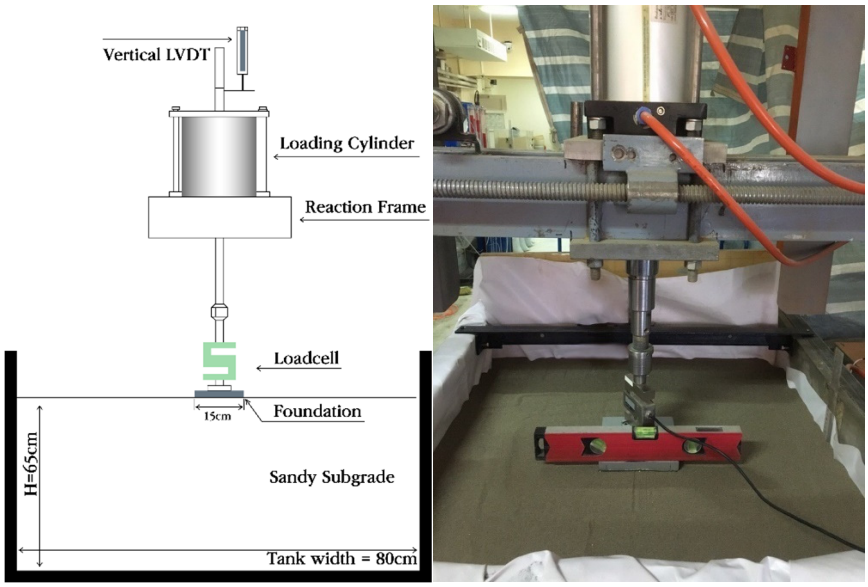

Figure 3. Schematic and actual picture of the bearing capacity physical model.

A standard vertical loading system was utilized to measure the bearing capacity of the square foundation on various subgrade conditions. After preparing the subgrade, the foundation model was attached to the vertical loading system and placed on the subgrade. The vertical force was applied to the foundation using a pneumatic jack, connected to the foundation through a load cell (see Figure 3). To monitor foundation settlements, an LVDT was used and fixed to the pneumatic cylinder's loading shaft. In the subgrade preparation, two distinct relative densities of 30 and 70% were chosen for each contamination percentage (0%, 5%, 10%, and 15%).

The amount of gas oil was calculated as a percentage of the weight of dry sand. To compensate for the evaporation during mixing, a slightly greater amount of gas oil was added to the mix. To achieve homogeneity and uniformity in the contamination distribution, gas oil was well mixed with the sand in a primary tank and then poured layer-by-layer in the main tank for preparation. Before the subgrade preparation, the required amount of sand to fill a specific volume was determined for each desired density. Inside the test tank, six layers of soil were marked with parallel horizontal lines. The determined soil mass for each layer was poured into the tank and compacted until it reached the specified height. Each layer consisted of 10 cm segments, with a fixed amount of sand poured, leveled, and compacted using a square tamper with a tamping area of 64 cm^2.

Two distinct relative densities (30% and 70%) were achieved using the same technique. Less effort was applied to compact the deeper layers, considering that they tend to densify further during the compaction of the top layers.

3. Test Program

To evaluate the effect of gas oil contamination on the model foundation's bearing capacity, tests have been systematically conducted at various gas oil contents and subgrade densities. Prior to the main tests, a series of direct shear tests were conducted to gain an insight into the mechanical properties of the contaminated sand before initiating the time-consuming model tests. In Table 4, the test program is presented in detail.

Table 4. List of the conducted tests with respect to the sand condition.

Test ID	Subgrade Relative Density (%)	Gas Oil Content (%)	Degree of Saturation (%)
Bearing Capacity Tests			
BC0-L	30%	0%	0%
BC5-L	30%	5%	15.5%
BC10-L	30%	10%	31%
BC15-L	30%	15%	46%
BC0-D	70%	0%	0%
BC5-D	70%	5%	18%
BC10-D	70%	10%	36%
BC15-D	70%	15%	54%
Direct Shear Tests			
DS0-L	30%	0%	0%
DS5-L	30%	5%	15.5%
DS10-L	30%	10%	31%
DS15-L	30%	15%	46%
DS0-D	70%	0%	0%
DS5-D	70%	5%	18%
DS10-D	70%	10%	36%
DS15-D	70%	15%	54%

4. Results and Discussion

4.1. Direct Shear Test Results

Direct shear tests were performed on the clean and contaminated sand according to the test program presented in Table 4. Failure envelopes for the relative densities of 30 and 70% at different gas oil contents are presented in Figures 4a and 5a, respectively. Soil properties at the mentioned relative densities, as well as the values of the friction angle and the apparent cohesion for the different soil conditions, are presented in Table 5. In these experiments, failure was defined as the displacement at which the shear strength peaked; in the absence of a peak, the shear stress corresponding to the tangent intersection was adopted.

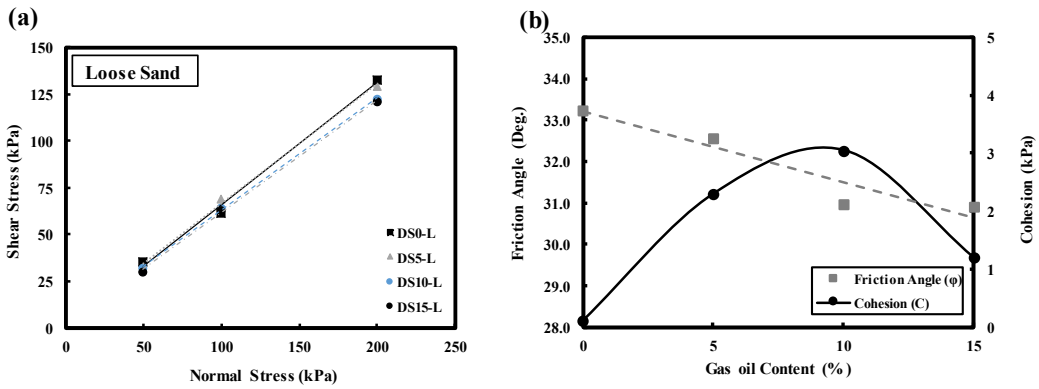

Figure 4. (**a**) Shear stress vs. normal stress; (**b**) Variation in the friction angle and apparent cohesion for loose samples at different gas oil contents.

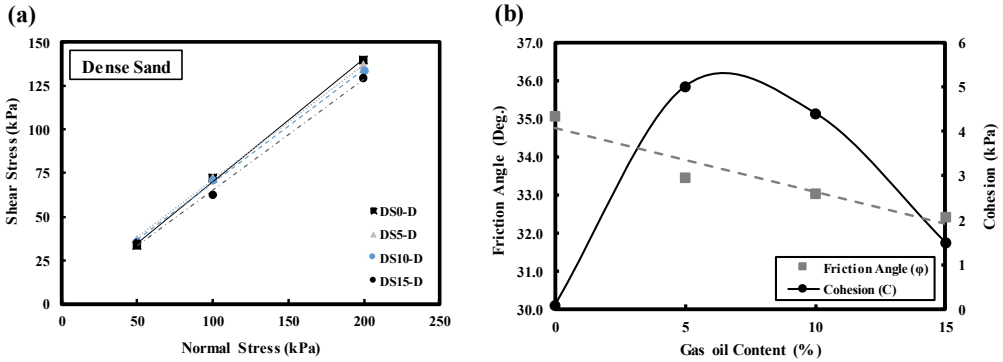

Figure 5. (**a**) Shear stress vs. normal stress; (**b**) Variation in friction angle and apparent cohesion for dense samples at different gas oil contents.

Table 5. Apparent cohesion and friction angle in different relative densities and gas oil contents.

Gas Oil Content (%)	Dr = 30%		Dr = 70%	
	γ_d = 14.19 (kN/m^3)	e = 0.866	γ_d = 15.14 (kN/m^3)	e = 0.749
	C (kPa)	φ (°)	C (kPa)	φ (°)
0	0.12	33.2	0.1	35.1
5	2.3	32.6	5	33.4
10	3.05	31	4.4	33
15	1.2	31	1.5	32.4

Friction angle and cohesion values corresponding to each gas oil content in loose and dense soil conditions are depicted in Figures 4b and 5b, respectively. Results indicate a generally decreasing trend in the sand's friction angle as the gas oil content increases, with the loose and dense sands experiencing a maximum of 7 and 8% decrease.

The decrease in the friction angle is primarily due to the lubricating effect of the hydrocarbon coating on the sand particles, which reduces the surface roughness, facilitates interparticle sliding and slipping, and consequently lowers the friction angle. The behavior of coarse-grained soils is greatly dependent on the physical interaction of the soil particles. Rajabi and Sharifipour [31] utilized scanning electron microscopy (SEM) images to examine sand contaminated with light crude oil, revealing significant effects on the sand's microstructure. These effects include the formation of a viscous hydrocarbon coating on sand particles and the infiltration of contaminants into the contact areas between the particles and the empty spaces within them. This coating notably influences the surface characteristics of sand particles, leading to a reduction in the friction angle. Moreover, the thickness of this coating increases with a higher hydrocarbon content, resulting in a more pronounced decrease in the friction angle. Additionally, Figures 4b and 5b show that, as expected, the friction angle increases with the increase in the soil's relative density in all gas oil contents tested.

Apparent cohesion, on the other hand, increased with an increase in the gas oil content to a certain point, and then decreased. As can be seen from Figures 4b and 5b, the cohesion of loose and dense sand reached 3.05 and 5 kPa at gas oil contents of 10 and 5%, respectively, and by further increasing the gas oil content to 15%, the cohesion dropped in both loose and dense samples. The increase in the cohesion of sandy soils contaminated with hydrocarbons has been frequently reported in previous studies [13–15,20]. They attributed this increase to the high dynamic viscosity of oil and its inherent cohesiveness.

Rajabi and Sharifipour [31] explained that the bonding created between particles due to hydrocarbon contamination can generate cohesion due to their adhesion capacities. This effect is more pronounced at lower contamination levels, where the amount of hydrocarbon does not significantly influence the frictional behavior of the sand particles. Thereafter, augmenting the hydrocarbon concentration thickens the contact layers and fills empty

sand pores, which weakens the frictional behavior and reduces the induced cohesion. In a related study, Jia et al. [49] proposed that hydrocarbon-induced cohesion within soil pores compensates for reduced particle roughness. This, in turn, leads to a stable trend in the soil shear strength, as the reduction in the friction angle combines with hydrocarbon-induced cohesion.

Although the viscosity-induced apparent cohesion might contribute to the increase in cohesion, a significant portion of the cohesion generated may be due to the suction generation as a result of the hydrocarbon contamination. The mechanism of apparent cohesion increase is quite similar to the suction-induced apparent cohesion in unsaturated soils, which is the highest at lower degrees of saturation and reduces as the saturation level increases. Hernández-Mendoza et al. [50] investigated the unsaturated shear strength of diesel-contaminated clayey soils. They reported a significant increase in the shear strength of diesel-contaminated soils compared to uncontaminated specimens, especially in large normal stresses. Their findings showed that this increase is due to an almost 150% increase in the total suction of the contaminated specimens compared to the uncontaminated specimens.

It can be seen that, compared to the loose samples, the dense samples reached their highest cohesion in a smaller gas oil content. This is primarily due to the fact that the suction-induced cohesion is greatly dependent on the void ratio of the soil samples [26,51]. Cui et al. [52] have also shown that the oil retention and transport properties are greatly dependent on the density and water content of the polluted soil. As dense samples have a smaller void ratio, the saturation degree increases with a smaller amount of gas oil, the sand mass reaches its suction peak at smaller gas oil contents, and the suction drop starts at smaller gas oil contents.

4.2. Physical Modeling Test Results

Physical model tests have been conducted for two respective subgrade densities as well. Figure 6a,b present the load–settlement relationships at different gas oil contents and relative densities. In these experiments, the ultimate bearing capacity is defined as the displacement at which the applied load peaks; in the absence of a peak, the load corresponding to the tangent intersection was adopted [26]. According to this method, the ultimate bearing capacity of the foundations rested on the loose sand was determined using the tangent-intersection method, and the ultimate bearing capacity of all foundations rested on the dense sand was determined from the peak value, except for the BC15-D test.

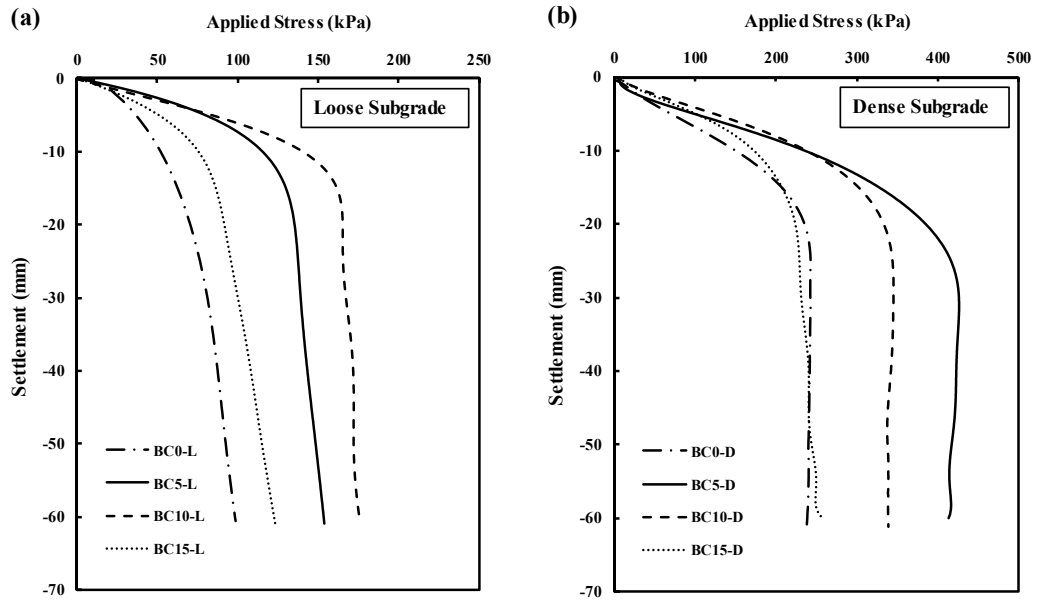

Figure 6. Applied stress versus footing settlement for (**a**) loose subgrade and (**b**) dense subgrade at different contamination contents.

Figure 7 displays the results of the bearing capacity ratio, which represents the ratio of the ultimate bearing capacity under varying gas oil contents to the ultimate bearing capacity under uncontaminated conditions. It can be seen in Figure 7 that, in the tests conducted on the loose subgrade, the bearing capacity of the foundation increases as the gas oil content increases in the BC5-L and BC10-L tests. After adding further gas oil to the mix, in the BC15-L test, the bearing capacity decreases significantly. As discussed earlier, despite a reduction in the friction angle of loose and dense sand, the cohesion of the samples increased significantly when mixed with 5% and 10% gas oil, and then dropped at higher gas oil contents.

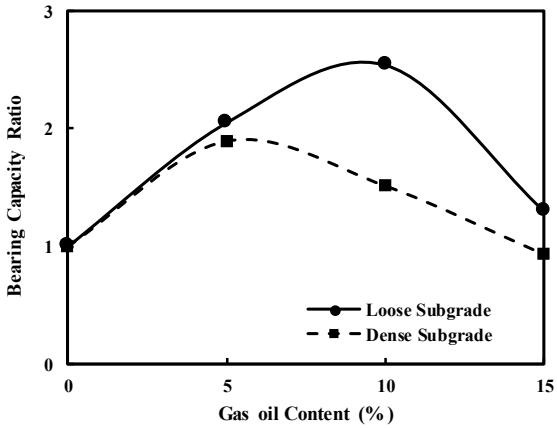

Figure 7. Variation in the bearing capacity of the foundation with respect to the subgrade density and contamination level.

The appearance of cohesion in the shear strength activates the cohesion term—previously absent in dry sand—in the bearing capacity equation, resulting in an increase in the bearing capacity of the foundation rested on the loose sand at the gas oil content of 5%. In this regard, the negative effects of the internal friction angle reduction and the positive effects of the cohesion increase on the bearing capacity of the foundation cancel one another in a way that results in an increase in the bearing capacity of the foundation. As discussed in the previous section, after passing the peak suction, mobilized in a certain gas oil content, the apparent cohesion reduces, which manifests itself as the reduction in the bearing capacity, as can be seen in Figure 7.

Based on the results presented in Figures 4b, 5b and 7, it can be seen that, among the different gas oil contents, the greatest ultimate bearing capacity is achieved at the gas oil content that exhibited the highest apparent cohesion in the direct shear test. That is to say, the highest bearing capacity is achieved at 10% and 5% gas oil content for the loose and dense sand, respectively, which is consistent with the results of the direct shear test indicating the highest cohesion at 10 and 5% gas oil content for the loose and dense sand, respectively.

The results show that implementing a worst-case scenario and overly conservative approach in the evaluation of the bearing capacity potential of foundations rested on hydrocarbon-contaminated sand might not always be a rational or efficient approach in the design or retrofit of such foundations, which can lead to unnecessarily cautious practices. In this respect, the actual conditions and scenarios in which the foundation bearing capacity could be jeopardized due to hydrocarbon contamination should be assessed before adopting conservative and expensive measures. It should also be noted that the cohesion term contribution to the bearing capacity of the foundation in this study might not be applicable in cases where very large or embedded foundations are designed, as other bearing capacity terms (i.e., the surcharge term and friction term) may become more influential, overshadowing the cohesion term effects. Moreover, the contamination of soils with hydrocarbons of high-lubrication potential (and possibly in low-apparent cohesion) might have more pronounced effects on the friction angle reduction and, consequently, make the friction term

more influential in the bearing capacity of foundations. Therefore, the interplay between different terms of the bearing capacity equation may lead to different results.

Figure 8a,b compare the calculated bearing capacity of the foundations using Terzaghi's general bearing capacity equation with the measured values for loose and dense subgrades, respectively. The data derived from the direct shear test have been used in the calculations. Bearing capacity factors (i.e., N_c, N_q, and N_γ) were adopted from Kumbhojkar [53], and the shape factors ζ_c and ζ_γ were calculated using the equations presented by the Vesic [54]. Previous studies have shown that the bearing capacity factor, N_γ, is dependent on the absolute width of the foundation for square and circular footings [45]. To account for the scale effects in the reduced-scale modeling, N_γ values were adopted based on the recommendations of Cerato and Lutenegger [45]. It can be seen in Figure 8a,b that the measured bearing capacity results are in acceptable agreement with those predicted based on Terzaghi's bearing capacity equation for general and local shear failure. Except for the BC0-D and BC15-D, all measured bearing capacity values fall in between the predicted local and general failure values.

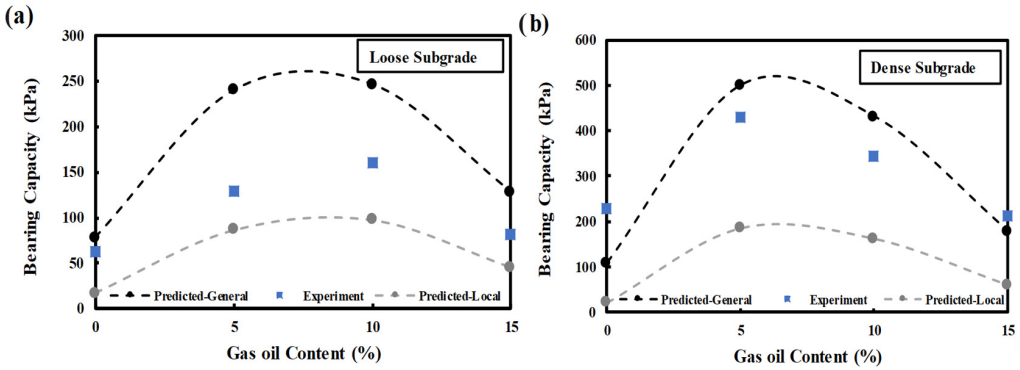

Figure 8. Comparison of the predicted local and general bearing capacity with the experimentally measured results for (**a**) loose subgrade and (**b**) dense subgrade at different gas oil contents.

Vesic [54,55] has comprehensively studied the failure modes of footings rested atop sand at different relative densities and embedment depths. Using model testing, Vesic [54] identified three load–settlement curves, each ascribed to general, local, and punch shear failures. General shear failure was attributed to the curves with a peak and a postpeak reduction in the bearing capacity and soil bulging around the loaded footing. Local shear failure, on the other hand, exhibited limited bulging around the loaded footing with a load–settlement curve consisting of a higher initial slope, followed by a less-steep or almost-flat slope segment. Furthermore, the punching failure was attributed to curves with constant or a relatively modest decreasing slope in the loose sand, with the exhibition of almost no bulging around the loaded footing. Vesic [54] has shown that model foundations rested on sand demonstrate general shear failure at relative densities of 72% to 100%, local shear failure at relative densities ranging from 35 to 72%, and punching shear failure at relative densities of about 0 to 35%. In the present study, the failure mechanism of the model footings can be studied based on the load–settlement curves presented in Figure 6a,b, the bearing capacity results shown in Figure 8a,b, and the images from the subgrade condition at the end of loading (Figure 9). In this regard, according to the load–settlement curves presented in Figure 6a, it can be inferred that, other than the BC0-L curve, which almost shows a punching shear failure, other curves (i.e., BC5-L, BC10-L, and BC15-L) indicate shear failure mechanisms resembling the description of local shear failure. The results presented in Figure 8a also show that the measured bearing capacity results are quite near the predicted local shear failure values for the loose subgrade.



(**a**) (**b**) (**c**)

Figure 9. Subgrade condition after loading (**a**) dry dense subgrade with apparent heave around the loaded area; (**b**) dense subgrade at a gas oil content of 5% exhibiting major bulging and heave around the loaded area; (**c**) dense subgrade at a gas oil content of 15% indicating minor bulging and heave around the loaded area.

Based on Figure 6b, for the dense sand, the general shear failure is the prevailing mechanism in all gas oil contents tested, except for BC15-D, which shows a load–settlement curve resembling that described for the local shear failure. The results presented in Figure 8b demonstrate that the measured bearing capacity is more inclined to the predicted general shear failure results. The failure mode of the dense subgrade can also be identified from the pictures taken at the end of the foundation loading. According to Figure 9a–c, it can be seen that the BC0-D and BC5-D exhibit major soil bulging and heave around the loaded foundation, indicating general shear failure; whereas, in Figure 9c, a modest subgrade bulging and heave manifested, which is similar to the description of the local shear failure proposed by Vesic [54].

5. Conclusions

The present study investigates the effects of gas oil contamination on the bearing capacity and shear strength of coastal sand in varying relative densities and gas oil contents. Direct shear testing and bearing capacity physical modeling have been utilized to study contaminated sand's behavior. As anticipated, increasing the relative density led to higher friction angles and, in turn, improved the foundation's bearing capacity for all gas oil contents studied.

Physical modeling results demonstrated that the bearing capacity initially increases with the gas oil content up to a certain point, and then decreases. This pattern aligns with the findings of the direct shear tests, which show a substantial increase in the apparent cohesion up to a specific gas oil content. The direct shear tests also indicated that the lubrication of the sand particles due to gas oil contamination brought about an 8% reduction in the friction angle. Conversely, a significant increase in the apparent cohesion (attributed to soil suction) was observed, with an almost 5 kPa increase.

Furthermore, the physical modeling test results in different gas oil contents align reasonably well with predictions based on Terzaghi's general bearing capacity equation for both local and general shear failure. Improved precision can be achieved by correctly identifying the failure mode and using appropriate bearing capacity factors in the prediction equation. It is noteworthy that the measured bearing capacity of dense sand indicated general shear failure, while the loose subgrade leaned towards local shear failure. Additionally, it was observed that the dense sand exhibited maximum apparent cohesion and bearing capacity at a lower gas oil content compared to the loose sand.

The results from both this study and prior research lead to the conclusion that the strength properties of hydrocarbon-contaminated soils are heavily dependent on the soil's properties and the type of hydrocarbon contamination. This study, in particular, highlights the notable influence of the relative density and saturation level on the mechanical behavior of hydrocarbon-contaminated sands. Therefore, it can be inferred that hydrocarbon

contamination may not always diminish the strength properties and bearing capacity of sands. Different parameters should be carefully assessed before taking highly conservative approaches in the design and retrofit of foundations rested on unsaturated hydrocarbon-contaminated soils.

Author Contributions: Conceptualization, A.K. and M.M.; methodology, A.K., M.M. and H.P.; investigation, A.K., M.M., H.P. and D.L.; resources, D.L.; writing—original draft preparation, A.K. and H.P.; writing—review and editing, A.K., M.M. and D.L.; visualization, A.K. and H.P.; supervision, D.L.; project administration, D.L.; funding acquisition, D.L. All authors have read and agreed to the published version of the manuscript.

Funding: This work was supported by the Human Resources Development of the Korea Institute of Energy Technology Evaluation and Planning (KETEP) grant funded by the Korean government (Ministry of Trade, Industry and Energy) (no. 20214000000180), and the Korea Institute of Energy Technology Evaluation and Planning (KETEP) grant funded by the Korea government (MOTIE) (20224000000220, Jeonbuk Regional Energy Cluster Training of human resources).

Institutional Review Board Statement: Not applicable.

Informed Consent Statement: Not applicable.

Data Availability Statement: Data presented is contained within the article.

Conflicts of Interest: The authors declare no conflict of interest.

Abbreviations

CBR	California bearing ratio	B	Foundation width
USC	Unconfined compression strength	e_{min}	Minimum void ratio
Cu	Uniformity coefficient	e_{max}	Maximum void ratio
Cc	Coefficient of curvature	γ_{dmax}	Maximum dry unit weight
CL	Lean clay	γ_{dmin}	Minimum dry unit weight
ML	Silt	G_{Max}	Maximum shear modulus
SM	Silty sand	LVDT	Linear variable differential transformer
SP	Poorly graded sand	N_γ, N_q, N_c	Bearing capacity factors
SC	Clayey sand	ζ_c , ζ_γ,	Shape factors
Gs	Specific gravity		

References

1. Kermani, M.; Ebadi, T. The effect of oil contamination on the geotechnical properties of fine-grained soils. *Soil Sediment Contam. Int. J.* **2012**, *21*, 655–671. [CrossRef]
2. Al-Sanad, H.A.; Eid, W.K.; Ismael, N.F. Geotechnical properties of oil-contaminated Kuwaiti sand. *J. Geotech. Eng.* **1995**, *121*, 407–412. [CrossRef]
3. Lee, M.; Jung, J.-Y. Pollution risk assessment of oil spill accidents in Gararim Bay of Korea. *Mar. Pollut. Bull.* **2015**, *100*, 297–303. [CrossRef] [PubMed]
4. Yim, U.H.; Hong, S.; Lee, C.; Kim, M.; Jung, J.-H.; Ha, S.Y.; An, J.G.; Kwon, B.-O.; Kim, T.; Lee, C.-H.; et al. Rapid recovery of coastal environment and ecosystem to the Hebei Spirit oil spill's impact. *Environ. Int.* **2019**, *136*, 105438. [CrossRef]
5. National Geographic Information Institute. Environmental Issues and Actions. Available online: http://nationalatlas.ngii.go.kr/pages/page_2391.php (accessed on 25 September 2023).
6. Kang, C.-U.; Kim, D.-H.; Khan, M.A.; Kumar, R.; Ji, S.-E.; Choi, K.-W.; Paeng, K.-J.; Park, S.; Jeon, B.-H. Pyrolytic remediation of crude oil-contaminated soil. *Sci. Total. Environ.* **2020**, *713*, 136498. [CrossRef]
7. Shin, E.C.; Das, B.M. Bearing capacity of unsaturated oil-contaminated sand. *Int. J. Offshore Polar Eng.* **2001**, *11*, 220–226.
8. Nasr, A.M.A. Experimental and Theoretical Studies for the Behavior of Strip Footing on Oil-Contaminated Sand. *J. Geotech. Geoenviron. Eng.* **2009**, *135*, 1814–1822. [CrossRef]
9. Joukar, A.; Boushehrian, A.H. Experimental Study of Strip Footings Rested on Kerosene Oil- and Gas Oil-Contaminated Sand Slopes. *Iran. J. Sci. Technol. Trans. Civ. Eng.* **2020**, *44*, 209–217. [CrossRef]
10. Abtahi, S.; Hajiani Boushehrian, A. Experimental behavior of circular foundations on oil-contaminated sand. *Sci. Iran.* **2020**, *27*, 80–87. [CrossRef]
11. Al-Adly, A.I.F.; Fadhil, A.I.; Fattah, M.Y. Bearing Capacity of Isolated Square Footing Resting on Contaminated Sandy Soil. *Egypt. J. Pet.* **2019**, *28*, 281–288. [CrossRef]

12. Puri, V.K. Geotechnical aspects of oil-contaminated sands. *J. Soil Contam.* **2000**, *9*, 359–374. [CrossRef]
13. Nasehi, S.A.; Uromeihy, A.; Nikudel, M.R.; Javadi, A.A. Influence of Gas Oil Contamination on Geotechnical Properties of Fine and Coarse-Grained Soils. *Geotech. Geol. Eng.* **2016**, *34*, 333–345. [CrossRef]
14. Ahmadi, M.; Ebadi, T.; Maknoon, R. Effects of crude oil contamination on geotechnical properties of sand-kaolinite mixtures. *Eng. Geol.* **2021**, *283*, 106021. [CrossRef]
15. Khosravi, E.; Ghasemzadeh, H.; Sabour, M.R.; Yazdani, H. Geotechnical properties of gas oil-contaminated kaolinite. *Eng. Geol.* **2013**, *166*, 11–16. [CrossRef]
16. Srivastava, R.K.; Pandey, V.D. Geotechnical evaluation of oil-contaminated soil. In *Contaminated and Derelict Land the Proceedings of Green 2: The Second International Symposium on Geotechnics Related to the Environment Held in Krakow, Poland, September 1997*; Telford: London, UK, 1998.
17. Akinwumi, I.I.; Diwa, D.; Obianigwe, N. Effects of crude oil contamination on the index properties, strength and permeability of lateritic clay. *Int. J. Appl. Sci. Eng. Res.* **2014**, *3*, 816–824.
18. Akinwumi, I.I.; Maiyaki, U.R.; Adubi, S.A.; Daramola, S.O.; Ekanem, B.B. Effects of waste engine oil contamination on the plasticity, strength and permeability of lateritic clay. *Int. J. Sci. Technol. Res.* **2014**, *3*, 331–335.
19. Alhassan, H.M.; Fagge, S.A. Effects of crude oil, low point pour fuel oil and vacuum gas oil contamination on the geotechnical properties sand, clay and laterite soils. *Int. J. Eng. Res. Appl.* **2013**, *3*, 1947–1954.
20. Khamehchiyan, M.; Charkhabi, A.H.; Tajik, M. Effects of crude oil contamination on geotechnical properties of clayey and sandy soils. *Eng. Geol.* **2007**, *89*, 220–229. [CrossRef]
21. Sadiq, A.; Fattah, M.Y.; Aswad, M.F. Enhancement of the Acid Resistance of Silty Clay Using Nano-Magnesium Oxide. *Materials* **2023**, *16*, 5035. [CrossRef]
22. Kererat, C. Effect of oil-contamination and water saturation on the bearing capacity and shear strength parameters of silty sandy soil. *Eng. Geol.* **2019**, *257*, 105138. [CrossRef]
23. Rajabi, H.; Sharifipour, M. Influence of weathering process on small-strain shear modulus (Gmax) of hydrocarbon-contaminated sand. *Soil Dyn. Earthq. Eng.* **2018**, *107*, 129–140. [CrossRef]
24. Oh, W.T.; Vanapalli, S.K. Modelling the applied vertical stress and settlement relationship of shallow foundations in saturated and unsaturated sands. *Can. Geotech. J.* **2011**, *48*, 425–438. [CrossRef]
25. Oh, W.T.; Vanapalli, S.K.; Puppala, A.J. Semi-empirical model for the prediction of modulus of elasticity for unsaturated soils. *Can. Geotech. J.* **2009**, *46*, 903–914. [CrossRef]
26. Vaseghi Maghvan, S.; Imam, R.; McCartney, J.S. Relative density effects on the bearing capacity of unsaturated sand. *Soils Found.* **2019**, *59*, 1280–1291. [CrossRef]
27. Steensen-Bach, J.; Foged, N.; Steenfelt, J. Capillary induced stresses–fact or fiction? *Eur. Conf. Soil Mech. Found. Eng.* **1987**, *9*, 83–89.
28. Vanapalli, S.K.; Mohamed, F.M. Bearing capacity of model footings in unsaturated soils. In *Experimental Unsaturated Soil Mechanics*; Springer: Berlin/Heidelberg, Germany, 2007; pp. 483–493.
29. Uchaipichat, A. Prediction of shear strength for unsaturated soils under drying and wetting processes. *Electron. J. Geotech. Eng.* **2010**, *15*, 1087–1102.
30. Lau, C.; Bolton, M. The bearing capacity of footings on granular soils. II: Experimental evidence. *Geotechnique* **2011**, *61*, 639–650. [CrossRef]
31. Rajabi, H.; Sharifipour, M. Geotechnical Properties of Hydrocarbon-Contaminated Soils: A Comprehensive Review. *Bull. Eng. Geol. Environ.* **2019**, *78*, 3685–3717. [CrossRef]
32. *ASTM D-854-23*; Standard Test Methods for Specific Gravity of Soil Solids by Water Pycnometer. ASTM International: West Conshohocken, PA, USA, 1923.
33. *ASTM D-2488*; Standard Practice for Description and Identification of Soils (Visual-Manual Procedure). ASTM International: West Conshohocken, PA, USA, 2018.
34. *ASTM D-4253*; Standard Test Methods for Maximum Index Density and Unit Weight of Soils Using a Vibratory Table. ASTM International: West Conshohocken, PA, USA, 2019.
35. *ASTM D-4254*; Standard Test Methods for Minimum Index Density and Unit Weight of Soils and Calculation of Relative Density. ASTM International: West Conshohocken, PA, USA, 2016.
36. *ASTM D1298*; Standard Test Method for Density, Relative Density, or API Gravity of Crude Petroleum and Liquid Petroleum Products by Hydrometer Method. ASTM International: West Conshohocken, PA, USA, 2023.
37. *ASTM D445*; Standard Test Method for Kinematic Viscosity of Transparent and Opaque Liquids (and Calculation of Dynamic Viscosity). ASTM International: West Conshohocken, PA, USA, 2023.
38. *ASTM D86*; Standard Test Method for Distillation of Petroleum Products at Atmospheric Pressure. ASTM International: West Conshohocken, PA, USA, 2023.
39. *ASTM D93*; Standard Test Methods for Flash Point by Pensky-Martens Closed Cup Tester. ASTM International: West Conshohocken, PA, USA, 2020.
40. Verdugo, R.; Ishihara, K. The steady state of sandy soils. *Soils Found* **1996**, *36*, 81–91. [CrossRef]
41. Wood, F.M.; Yamamuro, J.A.; Lade, P.V. Effect of depositional method on the undrained response of silty sand. *Can. Geotech. J.* **2008**, *45*, 1525–1537. [CrossRef]

42. De Beer, E. Bearing capacity and settlement of shallow foundations on sand. In Proceedings of the Symposium on Bearing Capacity and Settlement of Foundation; Duke University: Durham, NC, USA, 1965; pp. 15–33.
43. Zhu, F.; Clark, J.I.; Phillips, R. Scale effect of strip and circular footings resting on dense sand. *J. Geotech. Geoenviron. Eng.* **2001**, *127*, 613–621. [CrossRef]
44. Shiraishi, S. Variation in Bearing Capacity Factors of Dense Sand Assessed by Model Loading Tests. *Soils Found.* **1990**, *30*, 17–26. [CrossRef]
45. Cerato, A.B.; Lutenegger, A.J. Scale effects of shallow foundation bearing capacity on granular material. *J. Geotech. Geoenviron. Eng.* **2007**, *133*, 1192–1202. [CrossRef]
46. Kusakabe, O. Foundations. In *Geotechnical Centrifuge Technology*; Taylor, R.N., Ed.; Blackie Academic & Professional: London, UK, 1995; pp. 118–167.
47. Vahedifard, F.; Robinson, J.D. Unified method for estimating the ultimate bearing capacity of shallow foundations in variably saturated soils under steady flow. *J. Geotech. Geoenviron. Eng.* **2016**, *142*, 04015095. [CrossRef]
48. Oh, W.T.; Vanapalli, S.K. Scale effect of plate load tests in unsaturated soils. *Int. J. Geomater* **2013**, *4*, 585–594.
49. Jia, Y.G.; Wu, Q.; Meng, X.; Yang, X.; Yang, Z.; Zhang, G. Case Study on Influences of Oil Contamination on Geotechnical Properties of Coastal Sediments in the Yellow River Delta. In *Advances in Environmental Geotechnics: Proceedings of the International Symposium on Geoenvironmental Engineering, Hangzhou, China, 8–10 September 2009*; Chen, Y., Zhan, L., Tang, X., Eds.; Springer: Berlin/Heidelberg, Germany, 2010; pp. 767–771. [CrossRef]
50. Hernández-Mendoza, C.E.; Ramírez, P.G.; Alegría, O.C. Geotechnical Evaluation of Diesel Contaminated Clayey Soil. *Appl. Sci.* **2021**, *11*, 6451. [CrossRef]
51. Esmat, Z.A.; Fadhil, A.I. Effect of relative density on the matric suction and its contribution to shear strength of unsaturated sandy soil. *Appl. Res. J.* **2016**, *2*, 134–142.
52. Cui, Y.J.; Delage, P.; Alzoghbi, P. Retention and transport of a hydrocarbon in a silt. *Géotechnique* **2003**, *53*, 83–91. [CrossRef]
53. Kumbhojkar, A. Numerical evaluation of Terzaghi's Nc. *J. Geotech. Eng.* **1993**, *119*, 598–607. [CrossRef]
54. Vesić, A.S. Analysis of ultimate loads of shallow foundations. *J. Soil Mech. Found. Div.* **1973**, *99*, 45–73. [CrossRef]
55. Vesic, A.B. Bearing capacity of deep foundations in sand. Highway research record. *Natl. Acad. Sci.* **1963**, *39*, 112–153.

Disclaimer/Publisher's Note: The statements, opinions and data contained in all publications are solely those of the individual author(s) and contributor(s) and not of MDPI and/or the editor(s). MDPI and/or the editor(s) disclaim responsibility for any injury to people or property resulting from any ideas, methods, instructions or products referred to in the content.